Accepted Manuscript

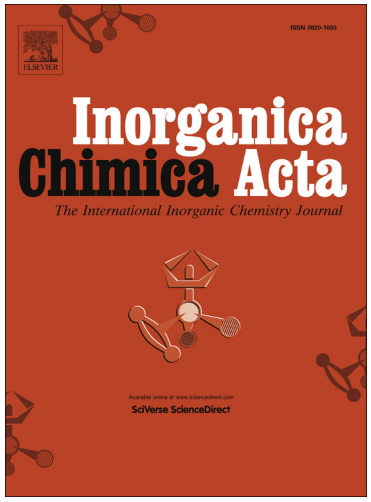

Palladium(II) and platinum(II) complexes of deprotonated N,N'-bis(2-pyridinecarboxamide)-1,2-benzene: synthesis, structural characterization and binding interactions with DNA and BSA

Titas Mukherjee, Buddhadeb Sen, Ennio Zangrando, Geeta Hundal, Basab Chattopadhyay, Pabitra Chattopadhyay

PII: S0020-1693(13)00223-5
DOI: http://dx.doi.org/10.1016/j.ica.2013.04.033
Reference: ICA 15438

To appear in: *Inorganica Chimica Acta*

Received Date: 18 December 2012
Revised Date: 20 March 2013
Accepted Date: 23 April 2013

Please cite this article as: T. Mukherjee, B. Sen, E. Zangrando, G. Hundal, B. Chattopadhyay, P. Chattopadhyay, Palladium(II) and platinum(II) complexes of deprotonated N,N'-bis(2-pyridinecarboxamide)-1,2-benzene: synthesis, structural characterization and binding interactions with DNA and BSA, *Inorganica Chimica Acta* (2013), doi: http://dx.doi.org/10.1016/j.ica.2013.04.033

This is a PDF file of an unedited manuscript that has been accepted for publication. As a service to our customers we are providing this early version of the manuscript. The manuscript will undergo copyediting, typesetting, and review of the resulting proof before it is published in its final form. Please note that during the production process errors may be discovered which could affect the content, and all legal disclaimers that apply to the journal pertain.

ACCEPTED MANUSCRIPT

Palladium(II) and platinum(II) complexes of deprotonated N,N'-bis(2-pyridinecarboxamide)-1,2-benzene: synthesis, structural characterization and binding interactions with DNA and BSA

Titas Mukherjee[a], *Buddhadeb Sen*[a], *Ennio Zangrando*[b], *Geeta Hundal*[c], *Basab Chattopadhyay*[d], *and Pabitra Chattopadhyay*[a]*

[a]*Department of Chemistry, Burdwan University, Golapbag, Burdwan-713104, India*
[b]*Dipartimento di Scienze Chimiche e Farmaceutiche, Via Licio Giorgieri 1, 34127 Trieste, Italy*
[c]*Department of Chemistry, Guru Nanak Dev University, Amritsar-143005, India*
[d]*Department of Solid State Physics, Indian Association for the Cultivation of Science, Jadavpur, Kolkata 700032, India*

Abstract

Two neutral complexes [ML] (where M = Pd (**1a**) and Pt (**1b**), L = bis(pyridine-2-carboxamide)benzene dianion) have been synthesized and characterized by physico-chemical and spectroscopic tools along with the detailed structural analysis by single crystal X-ray crystallography and theoretical (DFT) study. In solid state the compounds are isomorphous and isostructural showing the formation of $[ML]_3.3H_2O$ trimeric species. Electrochemical study of **1a** showed a quasi-reversible reductive response at $E_{1/2}$ = –1.148 V assignable to the Pd(II)/Pd(I) couple, while a metal centered irreversible oxidative peak centred at +0.977 V was observed in the voltammogram of **1b.** The interaction of the complexes with CT-DNA has been investigated using spectroscopic tools and viscosity measurement. In each case the association constant (K_b) was deduced from the absorption spectral study and the number of binding sites (n) and the binding constant (K) were calculated from relevant fluorescence quenching data, suggesting a non-covalent interaction between the metal complex and DNA, which could be assigned to an intercalative binding. In addition, the interaction of **1a** and **1b** was ventured with bovine serum albumin (BSA) with the help of absorption and fluorescence spectroscopy measurements. Through these techniques, the apparent association constant (K_{app}) and the binding constant (K) could be calculated for each complex.

Keywords: Palladium(II) complex; platinum(II) complex; crystal structure; DNA and BSA binding study.

*Corresponding author: E-mail: pabitracc@yahoo.com

ACCEPTED MANUSCRIPT

1. Introduction

The last few decades have witnessed a remarkable interest in pyridine carboxamide complexes in various fields of biological relevance like asymmetric catalysis, [1,2] dendrimer [3] and molecular receptor synthesis, **[**4] and also in the synthesis of compounds with possible antitumour properties [5]**.** The carboxamide [–C(O)NH–] group of the primary structure of proteins represents an important ligand construction unit in coordination chemistry, since its chelating rigid nature imparts a unique balance of stability versus reactivity, and has allowed for impressive developments in a variety of catalytic transformations.

Deprotonated amide groups readily coordinate metal ions through the amide-N and/or -O atom [6] forming a stable delocalized electronic system. The anticancer properties of *cis*platin and palladium(II) complexes stem from the ability of the *cis*-MCl_2 fragment to bind to DNA bases. However, *cis*platin also interacts with non-cancer cells, mainly binding molecules containing -SH groups, resulting in nephrotoxicity [7]. This has aroused interest in the design of novel palladium(II) [8] and platinum(II) complexes with better efficacy and lower toxicity. Serum albumins are the major soluble protein constituents of the circulatory system and serve as a depot- and as a transfer protein along with several physiological functions. BSA has been one of the most extensively studied of these proteins, particularly because of its structural homology with human serum albumin [9].

In the present work we have turned our attention to explore the amide functionality of the N,N'-bis(2-pyridinecarboxamide)-1,2-benzene ligand (H_2L) towards palladium(II) and platinum(II) ion. We report herein two novel Pd(II) (**1a**) and Pt(II) (**1b**) complexes with the tetradentate ligand having two deprotonated amide-N and two pyridinic-N donors. These species were structural characterized by X-ray diffraction and also by means of different physico-chemical, spectroscopic and computational studies. In addition, interaction of complexes **1a** and **1b** with CT-DNA and also with bovine serum albumin (BSA) have been studied. In order to establish the association mode of these small molecules to DNA, the binding (K_b) and the quenching constant (K_q) of the complexes with the double-helix has been determined from UV-Vis study and fluorescence displacement experiments using ethidium bromide as spectral probe. Beside this, the strong binding activity of complexes **1a** and **1b** with BSA was examined using absorption-fluorescence spectroscopy, further supported by viscosity measurements.

ACCEPTED MANUSCRIPT

2. Experimental

2.1. Materials and Instrumentation

All chemicals and reagents were obtained from commercial sources and used as received, unless otherwise stated. 2-Pyridinecarboxylic acid, 1,2-diaminobenzene and triphenyl phosphite were purchased from Aldrich and K_2PtCl_4 and $PdCl_2$ procured from Across, were used as such. The solvents used were purified following the standard procedures, all other chemicals used were of analytical reagent grade.

The elemental (C, H, N) analyses were performed on a Perkin Elmer model 2400 elemental analyzer. Electronic absorption spectra and IR spectra were obtained on a JASCO UV–Vis/NIR spectrophotometer model V-570 and on a Perkin-Elmer FTIR model RX1 spectrometer (KBr discs, 4000-300 cm^{-1}), respectively. ^1H NMR spectra were recorded on a Bruker AC300 spectrometer using TMS as an internal standard in DMSO-d_6 solvent. Electrospray ionization (ESI) mass spectra of complexes **1a** and **1b** were recorded with a QtofMicro Instrument (Waters, YA263). The fluorescence spectra complex bound to DNA were obtained at an excitation wavelength of 522 nm in the Fluorimeter (Hitachi-2000). Viscosity experiments were conducted on an Ostwald's viscometer, immersed in a thermostated water-bath maintained at 25 °C. Redox potentials were measured in CHI620D potentiometer in DMF using TBAP as supporting electrolyte at room temperature. Electrochemical setup was a three-electrode cell with glassy carbon, Ag/AgCl and a platinum wire as a working, reference and counter electrode, respectively. Molar conductances (Λ_M) were measured in a systronics conductivity meter 304 model in dimethylformamide at complex concentration of ~10^{-3} mol L^{-1}.

2.2. Preparation of the ligand

The ligand H_2L was synthesized following reported method [10] with slight modification. Pyridinic solution (10 ml) of 2-pyridinecarboxylic acid (1.23 g, 10 mmol) and 1,2-diaminobenzene (0.54 g, 5 mmol) was mixed under stirring condition followed by the dropwise addition of triphenyl phosphite (3.1 g, 10 mmol) at 80 °C for 4 hrs. and settled overnight. A pale brown crystalline solid resulted, was washed with methanol to give long white needles. Yield; 96%. Anal. Calc. for $C_{18}H_{14}N_4O_2$: C, 67.91; H, 4.43; N, 17.60. Found: C, 68.16; H, 3.94; N,

ACCEPTED MANUSCRIPT

1762.18. Anal. Calc.: IR (KBr, cm^{-1}): $\nu_{C=O,}$ 1677; $\nu_{NH,}$ 3317.9. ESI-MS (m/z): parent 318.11 (100 % abundance); $[M+H^+]$ 319.12 (19.7 % abundance).

2.3. Preparation of the complexes

*2.3.1. Synthesis of Pd(L) (**1a**)*

To a solution of H_2L (0.636 g, 0.50 mmol) in dry DMF (10 mL) was added NaH (0.0237 g, 1.00 mmol) and the resulting suspension was stirred for 30 min. To the resulting light yellow solution, $PdCl_2$ (0.089 g, 0.50 mmol) dissolved in DMF was added in portions with continuous stirring for a period of 3 h. The yellow precipitate resulted was filtered and washed with diethyl ether and vacuum dried. The residue was further dissolved in DMF (6.0 mL), filtered, and the volume of the filtrate was reduced to 3.0 mL. Yellow crystals, suitable for X-ray diffraction, were obtained by slow evaporation.

(**1a**).H_2O: $C_{18}H_{14}N_4PdO_3$: Anal. Calc.: C, 49.05; H, 3.20; N, 12.71. Found: C, 48.26; H, 3.94; N, 12.18. IR (KBr,cm^{-1}): $\nu_{C=O,}$ 1630; $\nu_{Pd-N,}$ 415. ESI-MS (m/z): $[M+Na^+]$, 463.01 (16 % abundance); $[M+H^+]$ 442.01 (96.2 % abundance). Conductivity (Λo, ohm^{-1} cm^2 mol^{-1}) in DMF: 51. UV-Vis in DMF, λ nm (ε) (ε, dm^3 $mol^{-1}cm^{-1}$): 281 (8,264), 305 (6,960). Yield: 65-68%.

*2.3.2. Synthesis of Pt(L) (**1b**)*

To a solution of H_2L (0.636 g, 0.50 mmol) in dry DMF (10.0 mL), NaH (0.0237 g, 1.00 mmol) was added and the resulting suspension was stirred for 30 min. To the resulting light yellow solution, aqueous K_2PtCl_4(0.2075 g, 0.50 mmol) was added in portions with vigorous stirring under nitrogen atmosphere and stirring has continued for further 10 h. The resulting orange-red solution was allowed to evaporate slowly, obtaining orange micro crystals suitable for X-ray diffraction studies.

(**1b**).H_2O: $C_{18}H_{14}N_4PtO_3$: Anal.: C, 40.83; H, 2.66; N, 10.58 Found: C, 40.67; H, 2.64; N, 10.54. IR (KBr, cm^{-1}): $\nu_{C=O,}$ 1637; $\nu_{Pt-N,}$ 435. ESI-MS (m/z): $[M+Na^+]$, 554.22 (20 % abundance); $[M+H^+]$, 532.22 (81 % abundance). Conductivity (Λo, ohm^{-1} cm^2 mol^{-1}) in DMF: 48. UV-Vis in DMF, λ nm (ε) (ε, dm^3 $mol^{-1}cm^{-1}$): 278 (5,142), 313 (5,564). Yield: 50-52 %.

ACCEPTED MANUSCRIPT

2.4. X-ray data collection and structural determination

Data collections of compounds **1a** and **1b** were carried at room temperature on a Bruker Smart Apex diffractometer equipped with CCD. (λ = 0.71073 Å). Cell refinement, indexing and scaling of the data sets were done by using programs Bruker Smart Apex and Bruker Saint packages. [11] The structures were solved by direct methods and subsequent Fourier analyses and refined by the full-matrix least-squares method based on F^2 with all observed reflections [12]. Hydrogen atoms were placed at calculated positions, those of lattice water molecules of compound **1b** were located on the ΔFourier map and analogously for molecule Ow1 of **1a**. All the calculations were performed using the WinGX System, Ver 1.80.05. [13] Crystal data and details of refinements are given in **Table 1**.

2.5. DNA binding studies of palladium(II) and platinum(II) complexes

The binding experiments with calf thymus DNA for complexes **1a** and **1b** were monitored following the same procedure previously reported by us [14] with UV-Vis and fluorescence spectroscopic tools and also by viscosity and cyclic voltammetry measurements.

All the experiments involving the interaction of the complexes with CT-DNA were carried out in MilliQ water containing Tris–HCl buffer (pH 8.04). The solution of CT-DNA in the buffer gave a ratio of UV absorbance of ca. 1.8 –1.9:1 at 260 and 280 nm, indicating that the CT-DNA was sufficiently free of protein [15]. Stock solution of DNA was always stored at 4 ºC in the dark and used within four days. The CT-DNA concentration per nucleotide was determined spectrophotometrically by employing an extinction coefficient of 6600 M^{-1} cm^{-1} at 260 nm [16]. The complexes were dissolved in a solvent mixture of 1% DMSO and 99% tris–HCl buffer at 1.0×10^{-4} M^{-1} concentration. Absorption spectral titration experiment was performed by keeping constant the concentration of the complex (10 µM) and varying the CT-DNA concentration. While measuring the absorption spectra, an equal amount of CT-DNA was added to both the complex solutions and the reference solution to take into account the absorbance of DNA itself.

In the emission quenching experiment, ethidium bromide (EB) was used as a common fluorescent probe for the DNA in order to examine the mode and process of metal complex binding to the double-helix [17]. A 5.0 µL of the EB tris–HCl buffer solution (1.0 mmol L^{-1}) was added to 1.0 mL of DNA solution (at saturated binding levels) [18], stored in the dark for 2 h.

ACCEPTED MANUSCRIPT

Then the solution of each of the Pd(II) and Pt(II) complexes was titrated into the DNA/EB mixture and diluted in tris–HCl buffer to 5.0 mL to get the solution with the appropriate complex/ CT-DNA mole ratio. After the incubation at room temperature for 30 min, the fluorescence spectra of EB bound to DNA were recorded (λ_{ex}= 522 nm) in the Hitachi 4500 Fluorimeter. All measurements were performed at ambient temperature.

The binding interaction of the metal complexes with DNA was studied by the well known method employing the Ostwald's viscometer. The CT-DNA solution (5 μM) was titrated with Pt(II) and Pd(II) complexes (0.5–3.5 μM), following the change of the viscosity in each case. Data are presented as $(\eta / \eta_0)^{1/3}$ versus the ratio of the concentration of the compound and CT-DNA, where η is the viscosity of CT-DNA in presence of the compound and η_0 is the viscosity of CT-DNA alone. Viscosity values were calculated from the observed flow time of CT-DNA-containing solution corrected from the flow time of buffer alone (t_0), $\eta = t\text{-}t_0$ [19].

2.6. Protein (BSA) binding experiments of palladium(II) and platinum(II) complexes

The binding study with bovine serum albumin (BSA) for complexes **1a** and **1b** were done dissolving the BSA in MilliQ water (1.0×10^{-5} M^{-1}) and the stock solutions of each of the complexes were prepared in DMSO-H_2O (1:99 v/v) mixture at 1.0×10^{-5} M^{-1} concentration. Both the absorption and fluorescence quenching experiments (λ_{ex}= 280 nm) were performed by gradually increasing the complex concentration, keeping fixed the concentration of BSA. All the experimental sets were carefully degassed purging pure nitrogen gas for 5 min.

2.7. Computational details

The DFT calculations for the isolated complexes **1a** and **1b** were performed using Dmol[3] code [20] in the framework of a generalized-gradient approximation (GGA) [21]. The geometry of the molecules were fully optimized using the hybrid exchange-correlation functional BLYP [22] and a double numeric plus polarization (DNP) basis set (Supplementary material, **Figs. s1-s3**). The electronic structures were also calculated at the same level. No constraints on bond lengths, bond angles or dihedral angles were applied in the calculations, and all atoms were free to optimize. Convergence was assumed to be reached when the total energy change between two consecutive self-consistent field (SCF) cycles was less than $1x10^{-5}$ a.u.

ACCEPTED MANUSCRIPT

3. Results and Discussion

3.1. Synthesis and characterization

The organic ligand L was synthesized by the reaction of 1, 2-diaminobenzene with 2-pyridinecarboxylic acid stirring at 80-85 °C in pyridine medium, and it has been characterized by IR and ^{1}H NMR spectral analyses. The palladium(II) and platinum(II) complexes **1a** and **1b** were obtained in good yield from the reaction of palladium(II) chloride and potassium tetrachloro platinate(II), respectively with the tetradentate ligand L in 1:1 molar ratio in the DMF medium with prolonged stirring at room temperature (*viz* **Scheme 1**).

The monomeric complexes **1a** and **1b** are soluble in DMF and DMSO but insoluble in methanol and ethanol. The conductivity measurement of complexes in DMF showed the conductance values in the range of 42-53 Λ_o mol^{-1} cm^{-1} at 300 K. These values suggest that the complexes exist as non-electrolytes in solution [23].

3.2. Structural description of **1a** *and* **1b**

The X-ray structural analysis show that complexes **1a** and **1b** are isomorphous and isostructural showing the formation of $[ML]_3.3H_2O$ aggregates (M = Pd and Pt, respectively L = bis(pyridine-2-carboxamide)benzene dianion. The independent crystallographic unit comprises of one and half neutral metal complex, being one located on a two-fold axis passing through the metal and bisecting the N_{amide}-M-N_{amide} bond angle, as shown in **Figs. 1** and **2** for the Pt derivative **1b**. The crystals contain also some disordered water lattice molecules.

As expected, in **1a** and **1b** the metal ion is chelated by the tetradentate dianionic ligand L in a square planar coordination geometry and due to the nature of the ligand all the atoms in each complex are coplanar. The bond lengths reported in **Table 2** indicate that the values relative to the pyridine N donors are significantly longer by ca. 0.1 Å than those of the amide nitrogen atoms, either in the Pd and Pt complexes, and the Pd-N bond values are in agreement with those reported in analogous complexes [24]. On the other hand the Pd-N bond lengths appear slightly longer with respect to the correspondent Pt-N values in agreement with the metal ionic radius.

It is worth noting of the supramolecular arrangement observed in these compounds, being the complexes arranged as trimeric entities where complex Pt2 (or Pd2) of C2 symmetry (**Figs. 1** and **s4**) is stacking in between a pair of two symmetry related Pt1 (or Pd1) units (**Figs. 3** and **s5**).

ACCEPTED MANUSCRIPT

Within this trimer the Pt metal ions in **1b** are separated by 3.2897(1) Å, in an almost collinear arrangement forming a Pt(1)-Pt(2)-Pt(1) angle of 178.64(1)°. The correspondent figures in **1a** are close comparable being of 3.2903(4) Å and 179.33(1)°, respectively. This packing feature is not unusual for square planar complexes having aromatic ligands and the aggregation of complexes are stabilized by a combination of π-π stacking interactions between the pyridine and phenyl rings of the ligands and d^8-d^8 metallophilic contacts. [25-27]. A structural indication of the latter interaction between the metals is the slight displacement from the N_4 donor set plane of atom M(1) by ca. 0.03 Å towards M(2) (M = Pt or Pd) inside each trimer. A rotation of *ca*. 140° is requested to complex Pt1 in order to be superimposed to Pt2 that occupies the center (**Fig. 3**), and similarly for the Pd complex.

Since the number of water molecules and crystal packing are close comparable for **1a** and **1b**, we limit here the description for the former compound. The lattice water molecules reside sideways to the trimer entities and are connected through H-bonds. In fact O2w, which is located on a two-fold axis, is weakly bound to O1w (O…O = 3.16 Å), which in turn connects the carbonyl oxygens O(1) and O(3) of symmetry related complexes (O….O = 2.80, 3.01 Å, respectively) forming a 2D packing arrangement parallel to the crystallographic *ab* plane.

3.3. Spectral properties

3.3.1. Electronic absorption spectral studies

The electronic absorption spectra of complexes **1a** and **1b** were recorded at room temperature using DMF as solvent. The spectra exhibit a sharp band around 280 nm assignable to the intramolecular $\pi \rightarrow \pi^*$ transition. Another relative high intensity band around 310 nm is due to a charge transfer from amide ligand core to metal, i.e. LMCT. The low energy tail of the charge transfer band that appears in the visible region of the spectrum is responsible for the yellow and orange-yellow color of the solution containing **1a** and **1b**, respectively. Here, it is observed that the transition for the palladium(II) complex shifted to lower energy compared to that of the platinum(II) derivative, and this study is in accordance with the theoretical calculation of the energy of HOMO and LUMO for **1a** and **1b**, being LUMO for complex **1a** lower lying compared to **1b** (**Fig. s3**).

ACCEPTED MANUSCRIPT

3.3.2. Electrochemistry

The electrochemical properties for **1a** and **1b** have been studied by cyclic voltammetry (CV) at a platinum working electrode in dimethylformamide (0.1 M TBAP as supporting electrolyte) at room temperature. The cyclic voltammograms of **1a** and **1b** are displayed in **Figs. 4** and **5**, respectively. The CV scan of **1a** revealed a one-electron quasi-reversible reductive response at $E_{1/2}$ = –1.148 V (E_{pc} = –1.245 V and E_{pa} = –1.051 V; ΔE = 194 mV) assignable to Pd(II)/Pd(I) couple. On the contrary, platinum(II) in **1b** is irreversibly oxidized to platinum(IV) by $2e^-$ stoichiometry [28, 29] centred at +0.977 V. From the theoretical calculation of HOMO and LUMO energy of both complexes, it may be derived that the comparatively lower energy of LUMO of **1a** may be responsible for the reduction of Pd(II)/Pd(I) and accordingly the higher energy of HOMO of **1b** for the irreversible oxidation of Pt(II) to Pt(IV) (**Fig. s3**).

3.4. Binding experiments with calf thymus-DNA

The mode of interaction of the complexes **1a** and **1b** with calf thymus DNA (CT-DNA) has been investigated using absorption and emission spectroscopic tools as well as by viscosity and cyclic voltammetry measurements.

3.4.1. Absorption spectroscopy

Electronic absorption spectroscopy is used as a distinctive characterization tool for examining the binding mode of metal complexes with DNA [18, 30]. In intercalative binding mode, the π* orbital of the intercalated ligand can couple with the π orbital of the base pairs, thus decreasing the π→π* transition energy and resulting in bathochromism. On the other hand, the coupling π orbital was partially filled by electrons, thus decreasing the transition probabilities and concomitantly resulting in hypochromism [31]. The absorption spectra of the free metal complexes and of their adducts with CT-DNA (at a constant concentration of the compounds) are given in **Figs. 6** and **s6** for complexes **1a** and **1b**, respectively. The extent of hyperchromism in the absorption band is generally consistent with the strength of intercalative interaction [28-31]. As the concentration of CT-DNA is increased, it was found that the Pd and Pt complexes at 270 nm and 268 nm exhibit hyperchromicity of 3.5/19.76% and 3.7/24.02%, respectively. This feature might be ascribed to the fact that both of the co-complexes could uncoil the helix structure of DNA and made more bases embedding in DNA exposed [32-34]. In order to

ACCEPTED MANUSCRIPT

establish the binding strength of the metal complexes with CT-DNA, the apparent association constant K_b was determined from the spectral titration data using the following equation [35]

$$1/\Delta\varepsilon_{ap} = 1/ (\Delta\varepsilon K_b D) + 1/\Delta\varepsilon$$

where, $\Delta\varepsilon_{ap}= |\varepsilon_a-\varepsilon_f|$, $\Delta\varepsilon= |\varepsilon_b-\varepsilon_f|$, D = [DNA], and ε_a, ε_b and ε_f are respectively the apparent, bound and free extinctions coefficient of each of the compound in respective cases. K_b, expressed as M^{-1}, is derived from the slope of the graph obtained by plotting the [DNA]/(ε_a-ε_f) *vs* [DNA] (**Fig. 7**). The K_b values for complexes for **1a** and **1b** were estimated to be $0.36 \times 10^4\ M^{-1}$ (R = 0.99999, n = 5 points) and $0.93\times 10^4\ M^{-1}$ (R = 0.99885, n = 5 points), respectively.

In order to corroborate the binding mode of intercalation of the Pd(II) and Pt(II) complexes with CT-DNA, we employed ethidium bromide (EB) that, interacting with DNA, represents a characteristic indicator of intercalation. The maximal absorption of EB at 479 nm decreased and shifted to 499 nm in presence of DNA (**Fig. s7**), typically indicating insertion between the base pairs [36]. The absorption spectra of the mixture solution of EB, palladium(II) complex **1a** and DNA and similarly for platinum(II) complex **1b** are reported as supplementary (**Figs. s7(a)** and **s7(b)**, respectively). The observed behavior could be indicative of: (1) being EB strongly bound to complex **1a** (or **1b**), the result is a decrease amount of EB intercalated into DNA; or (2) there exists a competition between the palladium(II) (or platinum(II)) complex and EB towards DNA intercalation, so releasing some free EB from DNA–EB complex. However, here the former account could be irrelevant because of the appearance of a new absorption band.

3.4.2. Fluorescence quenching analysis

The binding propensity of palladium and platinum complexes to CT-DNA has been analyzed by the steady-state emission quenching experiments using the emission intensity of ethidium bromide (EB). It is well known that EB can intercalate nonspecifically with DNA, causing a strong fluorescence. Other compounds competing with EB to intercalation in DNA will induce displacement of bound EB and a decrease in the fluorescence intensity. This fluorescence-based competition can provide indirect evidence for the DNA-binding mode. The fluorescence intensity of the EB/DNA system (with excitation wavelength of 522 nm) is reduced by the increasing concentration of the complexes (**Figs. 8** and **s8**), and caused by EB migration

ACCEPTED MANUSCRIPT

from a hydrophobic to an aqueous environment [37]. The quenching of EB bound to DNA by **1a** and **1b** is in agreement with the linear Stern–Volmer equation [38]:

$$I_0/I = 1 + K_q [Q]$$

where I_0 and I represent the fluorescence intensities in the absence and presence of quencher, respectively. K_q is a linear Stern–Volmer quenching constant, Q is the concentration of the quencher. In the quenching plot (insets of **Figs. 8** and **s8**) of I_0 /I *vs*. [complex], Kq is given by the ratio of the slope to the intercept. The K_q values are 0. 14×10^4 and 0.44×10^4 for complexes **1a** and **1b** respectively implies that both complexes can insert between DNA base pairs and that the platinum(II) complex can bind to DNA more strongly than the palladium(II) complex which is consistent with the absorption data.

The titration data obtained from the fluorescence experiment can be helpful also to calculate the number of binding sites and the apparent binding constant. In the following equation [39]:

$$\log[(I_0 - I)/I] = \log K + n \log[Q]$$

K and *n* represent the binding constant and number of binding sites of palladium complex to CT-DNA, respectively. The number of binding sites n, determined from the intercept of $\log[(I_0 - I)/I]$ *vs* log[Q] (**Fig. 9**), are 1.07 and 1.18 for **1a** and **1b**, respectively, indicating the existence of about a single binding site in DNA and a weaker association for the complexes. The K values were calculated to be 0.32×10^4 and 0.77×10^4 for **1a** and **1b**, respectively, with a trend similar to the apparent association constant values of the complexes.

3.4.3. Viscosity measurements

Since optical photophysical probes generally provide necessary, but insufficient clues to further clarify the interactions between the complex and DNA, viscosity measurements were carried out. Hydrodynamic measurements, sensitive to length change (i.e. viscosity and sedimentation), are regarded as the least ambiguous and the most critical tests of binding in solution in the absence of crystallographic structural data. A classical intercalation model demands that the DNA helix lengthens as base pairs are separated in order to accommodate the binding ligand, leading to an increase in DNA viscosity. In contrast, a partial, non-classical intercalation of compound could bend (or kink) the DNA helix, reducing its effective length and,

ACCEPTED MANUSCRIPT

concomitantly, its viscosity [19]. The results obtained in these viscosity measurement studies suggest that both the compounds **1a** and **1b** can intercalate between adjacent DNA base pairs, causing an extension of the helix with a concomitant increase of the DNA viscosity. The effects of both compounds on the viscosity of DNA are shown in **Fig. 10**.

3.5. Binding experiments with bovine serum albumin (BSA)

3.5.1. Absorption spectral characterization

The binding mode of complexes **1a** and **1b** with BSA were examined by electronic absorption titration with BSA. The absorption spectra of the free metal complexes and of their adducts with BSA are given in **Figs. 11** and **s9** for complex **1a** and **1b**, respectively. The spectra indicate a significant increase in the absorbance of BSA by increasing the concentration of the complex and are indicative of the fact that BSA adsorbs strongly the complex on its surface [40]. From these titration data the apparent association constant (K_{app}) of the complexes with BSA has been determined using the following equation [31]:

$$1/(A_{obs} – A_0) = 1/(A_c – A_0) + 1/ K_{app}(A_c – A_0)\,[comp]$$

where, A_{obs} is the observed absorbance of the solution containing different concentrations of the complex, A_0 and Ac are the absorbance of BSA and of the complex at 280 nm, respectively. The enhancement of the absorbance at 280 nm was attributable to the complex absorption at BSA surface. Based on the linear relationship between $1/(A_{obs} - A_0)$ *vs* the reciprocal concentration of the complex with a slope of $1/K_{app}(A_c - A_0)$ and an intercept equal to $1/(A_c - A_0)$ (**Fig**. **12**), the value of K_{app} was determined to be 1.262×10^5 M^{-1} (R = 0.99967, n = 5 points) and 1.402×10^5 M^{-1} (R = 0.99991, n = 5 points), for **1a** and **1b,** respectively.

3.4.2. Fluorescence quenching analysis

In the fluorescence quenching experiment, the fluorescence emission spectrum of BSA was studied increasing the concentration of the quencher (**Figs. 13** and **s10)**. The fluorescence quenching is described by the Stern–Volmer relation, [40] similarly as described above for CT-DNA binding experiments. From the slope of the regression line in the derived plot of I_0/I *vs* [complex] (insets of **Figs. 13** and **s10**) the K_q values for the complexes were determined to be

ACCEPTED MANUSCRIPT

4.29×10^4 for **1a** (R = 0.99825 for five points) and 4.62×10^4 for **1b** (R = 0.99948 for five points), indicating a strong affinity of both of the complexes to BSA.

4. Conclusions

Two novel square planar palladium(II) and platinum(II) complexes **1a** and **1b** of deprotonated tetradentate ligand N,N'-bis(2-pyridinecarboxamide)-1,2-benzene have been synthesized and characterized using various spectroscopic measurements. The X-ray structural characterization revealed that the palladiumd(II) and platinum(II) derivatives are isomorphous and are packed to form a trimeric motif with complexes connected by π-π interactions between the aromatic rings of the ligands and metallophilic bonding. The complexes have been found to interact with CT-DNA through an intercalative mode, which was investigated by absorption, fluorescence and viscosity measurement tools. The quenching rate constant, binding constant and number of binding sites were calculated according to the relevant fluorescence data. The binding constants indicate that the DNA-binding affinity, as well as the binding trend with BSA, increases from Pd(II) to Pt(II), in accordance with the relevant viscosity measurement study. The information obtained from the present work is indicative of the development of potential probes of DNA structure in future applications.

5. Supporting material

Crystallographic data for the structural analyses have been deposited with the Cambridge Crystallographic Data Centre, CCDC Nos. 856198 and 873080 for compounds **1a** and **1b**, respectively. Copies of this information are available on request at free of charge from CCDC, 12 Union Road, Cambridge, CB21EZ, UK (fax : +44-1223-336-033; e-mail: deposit@ccdc.ac.uk or http://www.ccdc.cam.ac.uk). MO diagrams from DFT calculations (**Figs. s1-s3**); ORTEP drawings of the independent units of **1a** (**Fig.s s4**, **s5**) and the spectral data of the binding interactions of complex **1b** with DNA and BSA (**Fig.s s6-s10**). Supplementary data associated with this article can be found, in the online version, at http:// XXXXXXX.

ACCEPTED MANUSCRIPT

Acknowledgements

Financial support from Council of Scientific and Industrial Research (CSIR), New Delhi, India is gratefully acknowledged. E. Zangrando thanks MIUR-Rome, PRIN 2007HMTJWP_002 for financial support.

References

[1] J. Lin, J.Y. Zhang, Y. Xu, X.K. Ke, Z. Guo, Acta Crystallogr. Sect. C 57 (2001) 192.

[2] B.M. Trost, I. Hachiya, J. Am. Chem. Soc. 120 (1998) 1104.

[3] J.D. Epperson, L.J. Ming, G.R. Baker, G.R. Newkome, J. Am.Chem. Soc. 123 (2001) 8583.

[4] S.R. Collinson, T. Gelbrich, M.B. Hursthouse, J.H.R. Tucker, Chem. Commun. (2001) 555.

[5] J. Zhang, Q. Liu, C. Duan, Y. Shao, J. Ding, Z. Miao, X. You, Z. Guo, J. Chem. Soc., Dalton Trans. (2002) 591.

[6] M. Nonoyama, S. Tomita, K. Yamasaki, Inorg. Chim. Acta 12 (1975) 33.

[7] J. Yoo, Y.S. Sohn, Y.K. Do**,** J. Inorg. Biochem. 73(1999) 187.

[8] J. Li, M.L. Zheng, I. King, T.W. Doyle, S.H. Chan, Curr. Med. Chem. 8 (2001) 121.

[9] X. M. He, D. C. Carter, Nature 358 (1992) 209.

[10] D.J. Barnes, R.L. Chapman, R.S. Vagg, E.C. Watton, J. Chem. Eng. Data, 23 (1978) 349.

[11] SMART, SAINT. Software Reference Manual; Bruker AXS Inc.: Madison, WI, 2000

[12] G. M. Sheldrick, Acta Cryst. A 64 (2008) 112.

[13] L. J. Farrugia, J. Appl. Crystallogr. 32 (1999) 837.

[14] T. Mukherjee, S. Sarkar, J. Marek, E. Zangrando, P. Chattopadhyay, Trans. Met. Chem. 37 (2012) 155.

[15] S. Satyanarayana, J.C. Dabrowiak, J.B. Chaires, Biochemistry 31 (1992) 9319.

[16] C.V. Kumar, E.H. Asuncion, J. Am. Chem. Soc., 115 (1993) 8541.

[17] C.V. Kumar, J.K. Barton, M.J. Turro, J. Am. Chem. Soc. 107 (1985) 5518.

[18] J.K. Barton, A.T. Danishefsky, J.M. Golderg, J. Am. Chem. Soc. 106 (1984) 2172.

[19] Y. Xiong, X.F. He, X.H. Zou, J.Z. Wu, X.M. Chen, L.N. Ji, R.H. Li, J.Y. Zhou and R.B. Yu, J. Chem. Soc. Dalton Trans., 1 (1999) 19.

[20] B. Delley, Phys. Rev. B 66 (2002) 155.

ACCEPTED MANUSCRIPT

[21] J.P. Perdew, K. Burke, M. Ernzerhof, Phys. Rev. Lett. 77 (1996) 3865.
[22] A.D. Becke, Phys. Rev. A 38 (1988) 3098.
[23] K. Dhara, P. Roy, J. Ratha, M. Manassero, P. Banerjee, Polyhedron 26 (2007) 4509.
[24] J.H. Lee, H.J. Kim, Y.W. Choi, Y.M. Lee, B. K. Park, C. Kim, S.-J. Kim, Y. Kim, Polyhedron 26 **(**2007) 1388.
[25] W.B. Connick, R.E. Marsh, W.P. Schaefer, H.B. Gray, Inorg. Chem. 36 (1997) 913.
[26] I.M. Sluch, A.J. Miranda, O. Elbjeirami, M.A. Omary, L.M. Slaughter, Inorg. Chem. 51 (2012) 10728.
[27] N. Marino, C.H. Fazen, J.D. Blakemore, C.D. Incarvito, N. Hazari, R.P. Doyle, Inorg. Chem. 50 (2011) 2507.
[28] M. Panda, S. Das, G. Mostafa, A. Castineiras, S. Goswami, Dalton Trans. (2005) 1249.
[29] S. Chattopadhyay, C. Sinha, P. Basu, A. Chakravorty, Organometallics 10 (1991) 1135.
[30] S.A. Tysoe, R.J. Morgan, A.D. Baker, T.C. Strekas, J. Phys. Chem. 97(1993) 1707.
[31] A.M. Pyle, J.P. Rehmann, R. Meshoyrer, C.V. Kumar, N.J. Turro, J.K. Barton, J. Am. Chem. Soc. 111 (1989) 3051.
[32] G. Pratviel, J. Bernadou, B. Meunier, Adv. Inorg. Chem. 45 (1998) 251.
[33] Q.L. Zhang, J.G. Liu, H. Xu, H. Li, J.Z. Liu, H. Zhou, L.H. Qu, L.N. Ji, Polyhedron 20 (2001) 3049.
[34] Z.S. Yang, Y.L. Wang, G.C. Zhao, Anal. Sci. 20 (2004) 1127.
[35] M. Baldini, M. Belicchi-Ferrari, F. Bisceglie, P. P. Dall Aglio, G. Pelosi, S. Pinelli, P. Tarasconi, Inorg. Chem. 43 (2004) 7170.
[36] W.D. Wilson, L. Ratmeyer, M. Zhao, L. Strekowski, D. Boykin, Biochemistry 32 (1993) 4098.
[37] Y.B. Zeng, N. Yang, W.S. Liu, J. Inorg. Biochem. 97 (2003) 258.
[38] M.R. Efink, C.A. Ghiron, Anal. Biochem. 114 (1981) 199.
[39] A. Kathiravan, R. Renganathan, Polyhedron 28 (2009) 1374.
[40] C. Chen, X. Qi, B. Zhou, J. Photochem. Photobiol. A: Chem. 109 (1997) 155.

ACCEPTED MANUSCRIPT

Figures' legend

Fig.1. ORTEP drawing (35% ellipsoid probability) of complex B of **1b** located on a crystallographic two-fold axis. (The same label scheme applies also to **1a**; primed atoms at -x, y, -z+1/2).

Fig. 2. ORTEP drawing (35% ellipsoid probability) of complex A of **1b**. (The same label scheme applies also to **1a**).

Fig. 3. Complex trimers in the crystal packing of **1b** connected through H-bonds occurring among carbonyl groups and lattice water molecules. A similar packing is observed in **1a**.

Fig.4. Cyclic voltammogram (scan rate 100 mV/s) of **1a** in DMF solution of 0.1 M TBAP, using platinum working electrode.

Fig.5. Cyclic voltammogram (scan rate 100 mV/s) of **1b** in DMF solution containing 0.1 M TBAP, using platinum working electrode

Fig.6. Electronic spectral titration of complex **1a** with CT-DNA at 271 nm in Tris-HCl buffer; [**1a**] = 2.62×10^{-5}; [DNA]: (a) 0.0, (b) 1.25×10^{-6}, (c) 2.5×10^{-6}, (d) 3.75×10^{6}, (e) 5.0×10^{-6} , (f) 6.25×10^{-6} mol L^{-1}. The arrow denotes the gradual increase of DNA concentration.

Fig. 7. Comparative plot of [DNA]/(ε_a-ε_f) *vs* [DNA] for the absorption titration of CT-DNA with complexes **1a** and **1b** in Tris-HCl buffer; association constant K_b: 0.36×10^4 M^{-1} (R = 0.99999, n = 5 points) for **1a**; 0.93×10^4 M^{-1} (R = 0.99885, n = 5 points) for **1b**.

Fig.8. Emission spectra of the CT-DNA-EB system in Tris-HCl buffer upon titration with complex **1a**. λ_{ex} = 522 nm; [EB] = 9.6×10^{-5}; [DNA] = 1.25×10^{-5}; [**1a**]: (a) 0.0, (b) 1.31×10^{-5}, (c) 2.62×10^{-5}, (d) 3.93×10^{-5}, (e) 5.24×10^{-5}, (f) 6.55×10^{-5} mol L^{-1}. The arrow denotes the gradual increase of complex concentration. Inset shows the plot of I_0/I *vs*. [**1a**]; $K_q = 0.16\times 10^4$ (R = 0.99876, n = 5 points)

Fig.9. Comparative plot of log[I_0-I/I] *vs*. log[complex] for the titration of CT-DNA-EB system with complexes **1a** and **1b** in tris-HCl buffer medium.

Fig.10. Effect of increasing amounts of Pd(II) and Pt(II) complexes on the relative viscosity of CT-DNA at 25 °C.

Fig.11. Absorption titration spectra of BSA in presence of complex **1a**. Concentration range of complex is 0-6.25×10^{-6} M^{-1}

ACCEPTED MANUSCRIPT

Fig. 12. The linear dependence of $1/A - A_0$ on the reciprocal concentration of complexes **1a** and **1b**.

Fig.13. Fluorescence quenching titration of BSA varying the concentrations of complex **1a**, [complex] = 0, 1, 2, 3, 4 and $5 \times 6.35 \times 10^{-6}$ M. Inset shows the Stern–Volmer plot.

Scheme 1. Synthetic routes of the complexes

ACCEPTED MANUSCRIPT

ACCEPTED MANUSCRIPT

Table 1. Crystallographic data for compounds **1a** and **1b**.

	1a.$1.5H_20$	**1b.**$1.5H_20$
Empirical Formula	$C_{54}H_{42}N_{12}O_9Pd_3$	$C_{54}H_{42}N_{12}O_9Pt_3$
Fw	1322.20	1588.27
Crystal system	Monoclinic	
Space group	*C* 2/c	
a, Å	14.5231(17)	14.5777(5)
b, Å	20.2671(17)	20.2335(6)
c, Å	16.4470(17)	16.4016(5)
β, deg	97.365(3)	97.237(2)
V, $Å^3$	4801.1(9)	4799.2(3)
Z	4	
*D*calcd, g cm^{-3}	1.829	2.198
μ (Mo-Kα) mm^{-1}	1.188	8.799
F(000)	2640	3024
θ range, deg	1.73 - 28.22	1.73 - 31.00
no. of reflns collcd	26979	36287
no. of indep reflns	5836	7530
R_{int}	0.0513	0.0325
no. of reflns (I>2σ(I))	3951	5593
no. of refined params	357	362
goodness-of-fit (F^2)	1.025	1.010
$R1$, $wR2$ (I >2σ(I)) [a]	0.0344, 0.0767	0.0231, 0.0487
R indices (all data)	0.0623, 0.0890	0.0428, 0.0554

[a] $R1 = \Sigma \, \big| \, |Fo| - |Fc| \, \big| \, / \, \Sigma \, |Fo|$, $wR2 = [\Sigma \, w \, (Fo^2 - Fc^2)^2 / \Sigma w \, (Fo^2)^2]^{½}$

ACCEPTED MANUSCRIPT

Table 2. Coordination bond lengths (Å) and angles (°) for compounds **1a** and **1b**.

	1a, M= Pd	**1b**, M= Pt
M(1)-N(1)	2.054(3)	2.040(3)
M(1)-N(4)	2.055(3)	2.044(2)
M(1)-N(2)	1.939(3)	1.953(2)
M(1)-N(3)	1.951(3)	1.944(3)
M(2)-N(5)	2.053(3)	2.043(3)
M(2)-N(6)	1.946(3)	1.958(2)
M(1)-M(2)	3.2903(4)	3.2897(1)
N(1)-M(1)-N(2)	81.33(10)	81.28(10)
N(1)-M(1)-N(3)	165.28(11)	165.79(10)
N(1)-M(1)-N(4)	112.51(10)	112.64(10)
N(2)-M(1)-N(3)	84.22(11)	84.81(10)
N(2)-M(1)-N(4)	166.13(11)	166.01(10)
N(3)-M(1)-N(4)	81.91(11)	81.22(10)
N(5)-M(2)-N(6)	81.85(11)	81.37(11)
N(5)-M(2)-N(6')	165.73(11)	165.90(10)
N(5)-M(2)-N(5')	112.41(15)	112.72(14)
N(6)-M(2)-N(6')	83.90(15)	84.55(15)
M(1)-M(2)-M(1')	179.33(1)	178.64(1)

Primed atoms at -x, y, -z+1/2.

ACCEPTED MANUSCRIPT

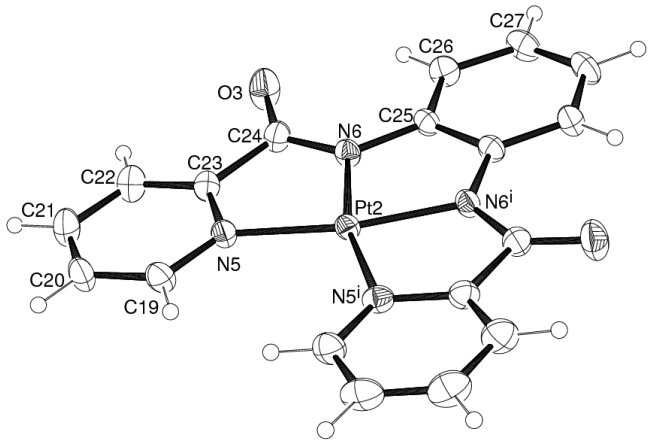

Fig. 1. ORTEP drawing (35% ellipsoid probability) of complex B of **1b** located on a crystallographic two-fold axis. (The same label scheme applies also to **1a**; primed atoms at -x, y, -z+1/2).

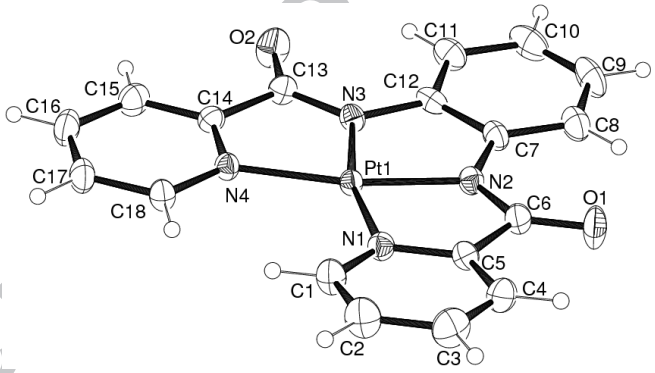

Fig. 2. ORTEP drawing (35% ellipsoid probability) of complex A of **1b**. (The same label scheme applies also to **1a**).

ACCEPTED MANUSCRIPT

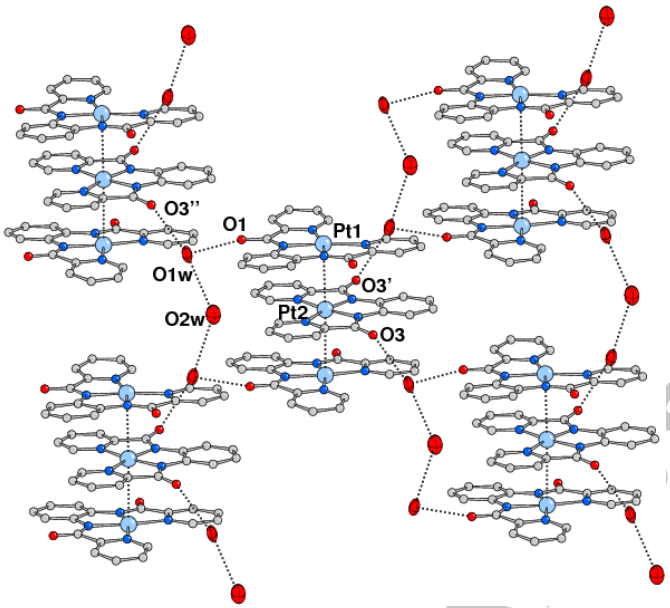

Fig. 3. Complex trimers in the crystal packing of **1b** connected through H-bonds occurring among carbonyl groups and lattice water molecules. A similar packing is observed in **1a**.

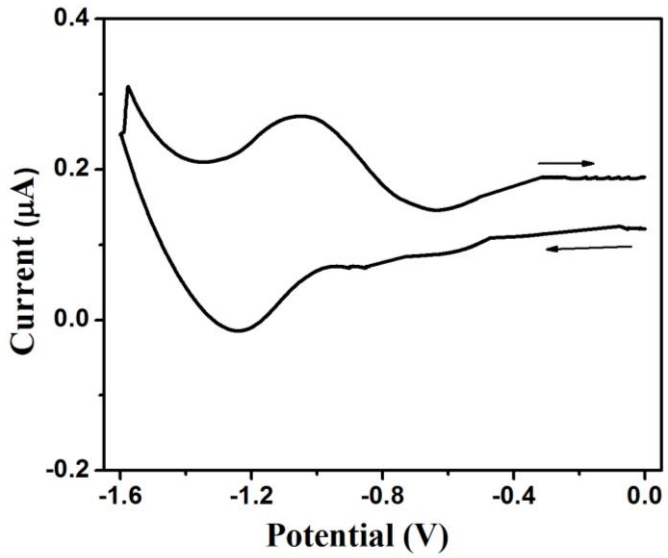

Fig.4. Cyclic voltammogram (scan rate 100 mV/s) of **1a** in DMF solution of 0.1 M TBAP, using platinum working electrode

ACCEPTED MANUSCRIPT

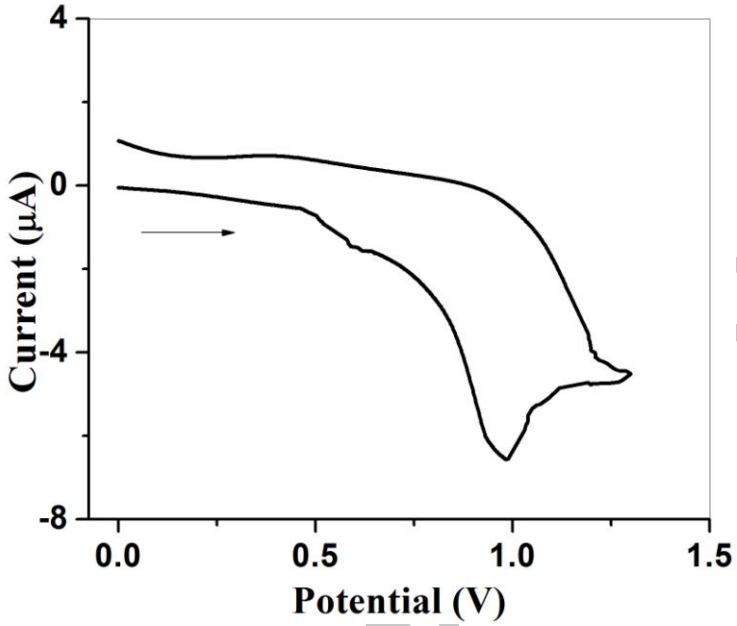

Fig.5. Cyclic voltammogram (scan rate 100 mV/s) of **1b** in DMF solution containing 0.1 M TBAP, using platinum working electrode

ACCEPTED MANUSCRIPT

ACCEPTED MANUSCRIPT

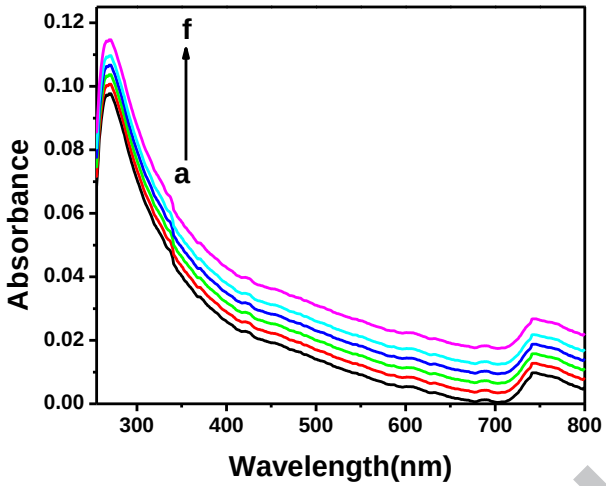

Fig.6. Electronic spectral titration of complex **1a** with CT-DNA in Tris-HCl buffer; [**1a**] = 2.62×10^{-5}; [DNA]: (a) 0.0, (b) 1.25×10^{-6}, (c) 2.5×10^{-6}, (d) 3.75×10^{6}, (e) 5.0×10^{-6} , (f) 6.25×10^{-6} mol L^{-1}. The arrow denotes the gradual increase of DNA concentration.

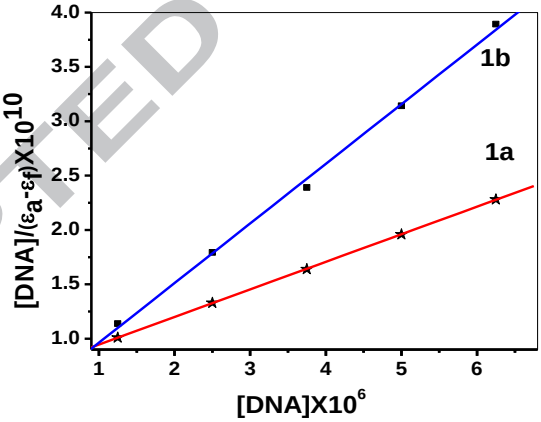

Fig. 7. Comparative plot of [DNA]/(ε_a-ε_f) *vs* [DNA] for the absorption titration of CT-DNA with complexes **1a** and **1b** in Tris-HCl buffer. Association constant K_b: 0.36×10^{4} M^{-1} (R = 0.99999, n = 5 points) for **1a**; 0.93×10^{4} M^{-1} (R = 0.99885, n = 5 points) for **1b**.

ACCEPTED MANUSCRIPT

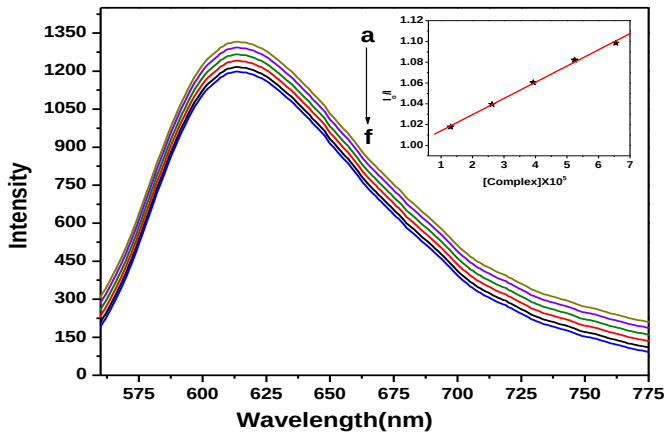

Fig.8. Emission spectra of the CT-DNA-EB system in Tris-HCl buffer upon titration with complex **1a**. λ_{ex} = 522 nm; [EB] = 9.6×10^{-5}, [DNA] = 1.25×10^{-5}; [**1a**]: (a) 0.0, (b) 1.31×10^{-5}, (c) 2.62×10^{-5}, (d) 3.93×10^{-5}, (e) 5.24×10^{-5}, (f) 6.55×10^{-5} mol L^{-1}. The arrow denotes the gradual increase of complex concentration. Inset shows the plot of I_0/I *vs*. [**1a**]; K_q = 0.16×10^4 (R = 0.99876, n = 5 points).

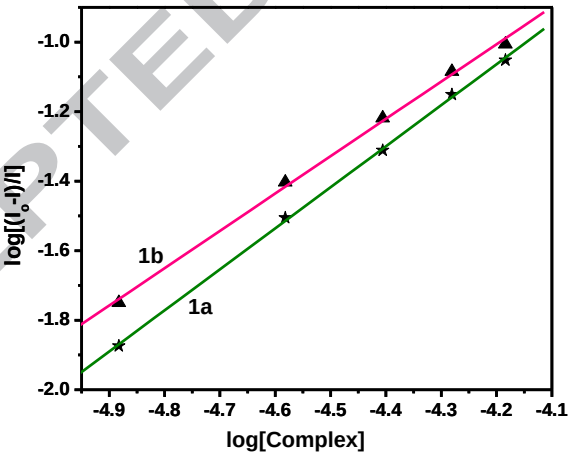

Fig. 9. Comparative plot of $\log[I_0\text{-}I/I]$ *vs*. log[complex] for the titration of CT-DNA-EB system with complexes **1a** and **1b** in tris-HCl buffer medium.

ACCEPTED MANUSCRIPT

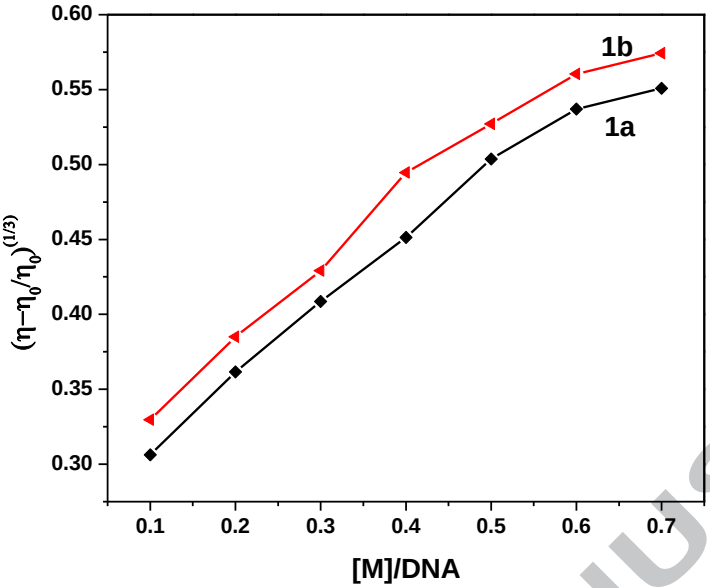

Fig. 10. Effect of increasing amounts of Pd(II) and Pt(II) complexes on the relative viscosity of CT-DNA at 25 °C.

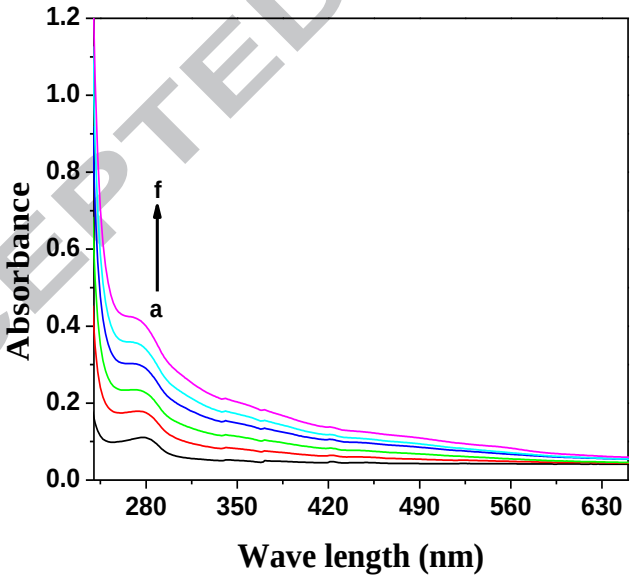

Fig. 11. Absorption titration spectra of BSA in presence of complex **1a**. Concentration range of the complex is 0-6.25× 10^{-6} M^{-1}.

ACCEPTED MANUSCRIPT

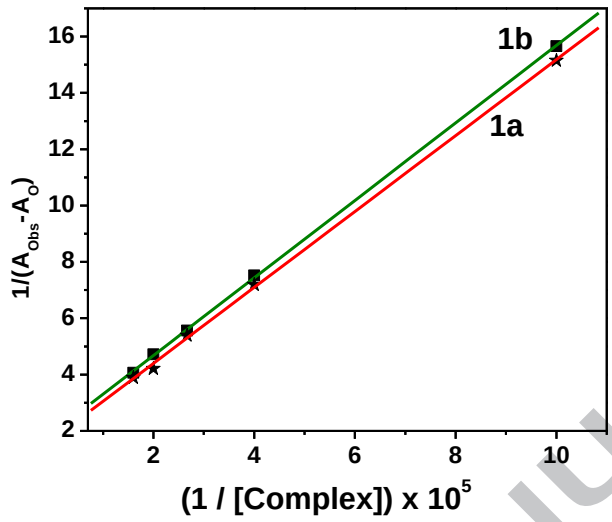

Fig. 12. The linear dependence of $1/A - A_0$ on the reciprocal concentration of **1a** and **1b**.

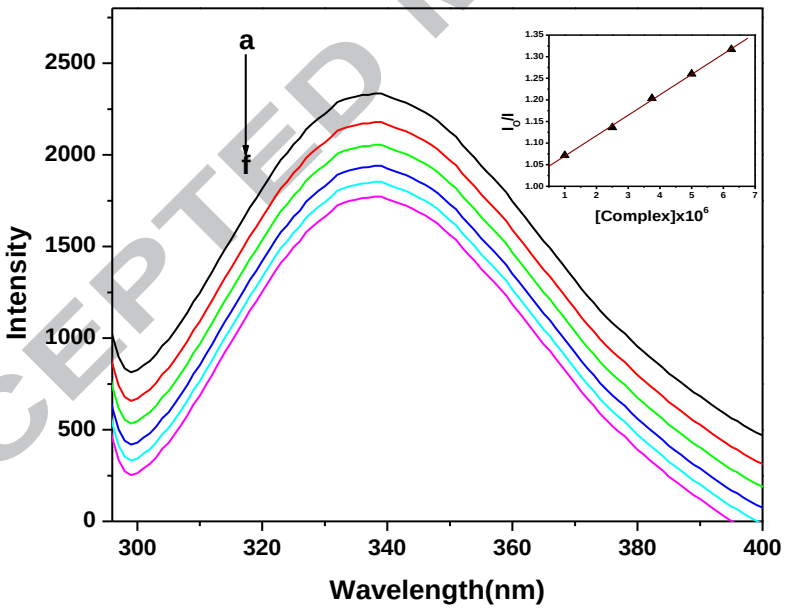

Fig. 13. Fluorescence quenching titration of BSA varying the concentration of **1a**, [complex] = 0, 1, 2, 3, 4 and 5 × 6.35 ×10^{-6} M. Inset shows the Stern–Volmer plot.

ACCEPTED MANUSCRIPT

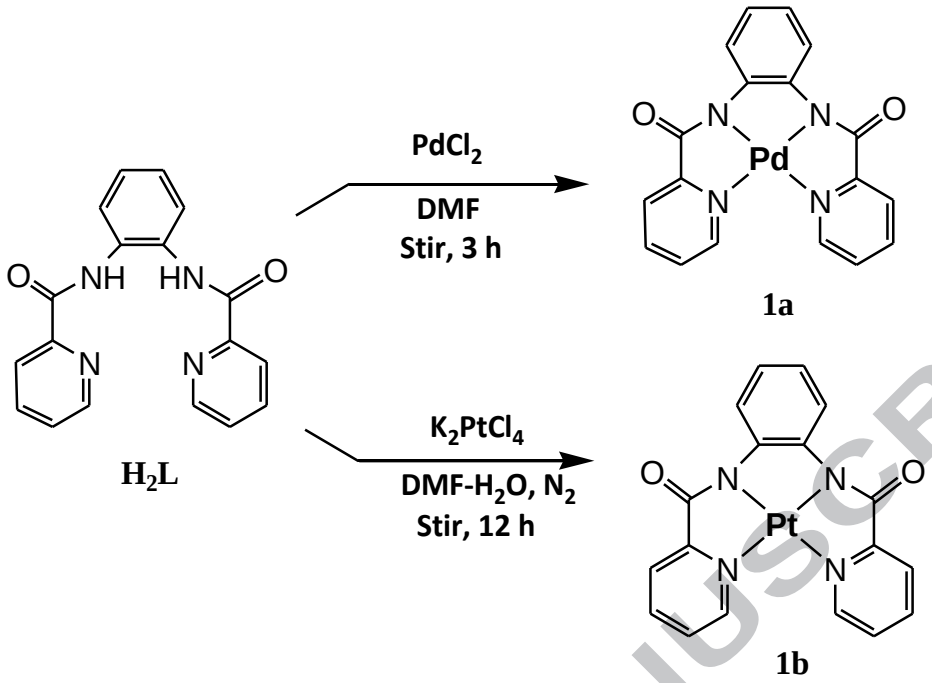

Scheme 1. Synthetic routes of the complexes

ACCEPTED MANUSCRIPT

ACCEPTED MANUSCRIPT

Highlights

- Two isomorphous and isostructural complexes of general formulation [ML].H_2O
- M= Pd (**1a**) and Pt (**1b**), L = bis(pyridine-2-carboxamide)benzene dianion)
- Synthesis, structural characterisation and redox behavior
- Spectroscopic study on the interaction of both **1a** and **1b** with CT-DNA and BSA
- Both complexes have strong noncovalent intercalative binding ability with CT-DNA

ACCEPTED MANUSCRIPT

ACCEPTED MANUSCRIPT

Graphical Abstract

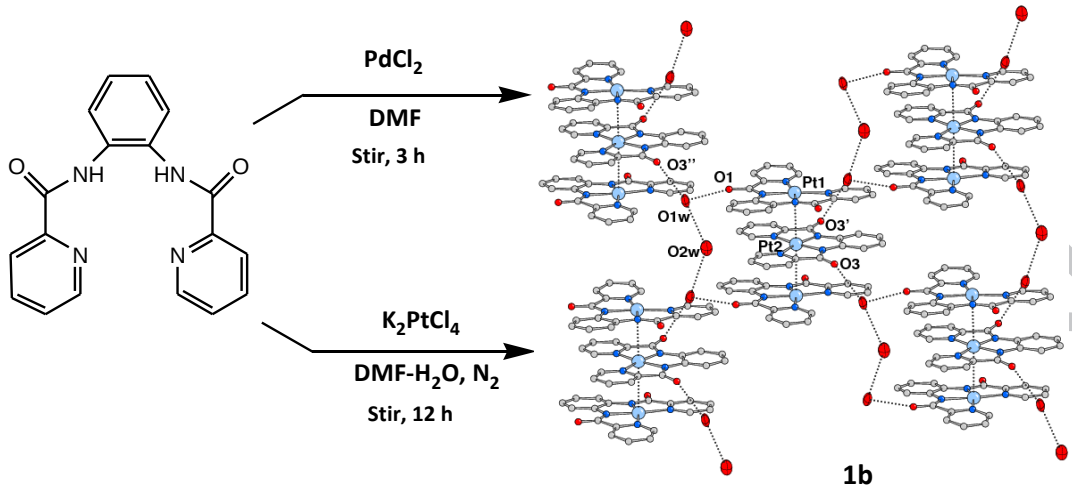

1b

for 1a Pt = Pd

ACCEPTED MANUSCRIPT

ACCEPTED MANUSCRIPT

Graphical Abstract (Synopsis)

Structurally characterized two isomorphous tetracoordinated palladium(II) and platinum(II) complexes of deprotonated carboxamide (**1a** and **1b**) have strong intercalative binding ability with CT-DNA through noncovalent bonding mode. The interactions of the complexes with bovine serum albumin (BSA) indicated the strong affinity of both of the complexes to BSA.

ACCEPTED MANUSCRIPT